Research Square

Preprints are preliminary reports that have not undergone peer review.
They should not be considered conclusive, used to inform clinical practice,
or referenced by the media as validated information.

Characterization of the Mitochondrial Genome of the Fruit-Eating Bat (Artibeus hirsutus)

María Fernanda Cruz Díaz
Instituto Politécnico Nacional
Jorge Ortega
Instituto Politécnico Nacional
Carlos F. Calderón-Palapa
fernandocalderonpalapa@gmail.com

Instituto Politécnico Nacional

Research Article

Keywords: Control region, Ka/Ks, Mitogenome, Phylogeny, Purifying selection, tRNA secondary structures

Posted Date: November 11th, 2026

DOI: https://doi.org/10.21203/rs.3.rs-11529747/v1

License: This work is licensed under a Creative Commons Attribution 4.0 International License.
Read Full License

Additional Declarations: No competing interests reported.

Characterization of the Mitochondrial Genome of the Fruit-Eating Bat (*Artibeus hirsutus*)

María Fernanda Cruz Díaz[1], Jorge Ortega[1], Carlos F. Calderón-Palapa[1*]

1. Laboratorio de Bioconservación y Manejo, Posgrado en Ciencias Químicobiológicas, Departamento de Zoología, Escuela Nacional de Ciencias Biológicas, Instituto Politécnico Nacional, Ciudad de México, Ciudad de México, México.

María Fernanda Cruz Díaz, mcruzd1703@alumno.ipn.mx, ORCID https://orcid.org/0009-0003-5766-2830

Jorge Ortega, artibeus2@aol.com, ORCID https://orcid.org/0000-0002-3623-0540

Carlos F. Calderón-Palapa, ccalderonp1900@alumno.ipn.mx, ORCID https://orcid.org/0009-0000-2101-2236

*Corresponding author: Carlos F. Calderón Palapa

Abstract

Background *Artibeus hirsutus* is a fruit-eating bat endemic to Mexico, distributed mainly along the Pacific slope and associated with tropical deciduous forests. Despite its broad regional distribution, the species is generally recorded at low abundances and remains one of the least studied members of the genus *Artibeus*. Genomic information available for this species is limited, particularly regarding its complete mitochondrial genome.

Methods and Results The complete mitochondrial genome of *A. hirsutus* was assembled and characterized using a wing membrane tissue sample (n = 1). The mitogenome was 16,670 bp long and consisted of 37 genetic elements: 13 protein-coding genes, 22 transfer RNA genes, and two ribosomal RNA genes, in addition to a 1,238-bp non-coding control region. Nucleotide composition showed an abundance of adenine and thymine, with an A+T content of 62.03%. Most transfer RNA genes retained the typical cloverleaf secondary structure, except for trnS1, which lacked the dihydrouridine (DHU) arm. All protein-coding genes exhibited nonsynonymous to synonymous substitution ratios (Ka/Ks) ratios below 1, consistent with purifying selection, whereas atp8 showed the highest Ka/Ks ratio. Phylogenetic analysis placed *A. hirsutus* within Stenodermatinae, clustering with other representatives of *Artibeus*.

Conclusions This study provides a comprehensive characterization of the mitogenome of *A. hirsutus* and expands the molecular resources available for the genus *Artibeus*. The information obtained provides a foundation for future comparative, phylogenetic, and population-level studies within Phyllostomidae.

Keywords: Control region, Ka/Ks, Mitogenome, Phylogeny, Purifying selection, tRNA secondary structures

Abbreviations: CR, control region; DHU, dihydrouridine; H, heavy strand; Ka/Ks, ratio of the rate of nonsynonymous substitutions to the rate of synonymous substitutions; L, light strand; PCG, protein-coding genes; rRNA, ribosomal RNA; tRNA, transfer RNA; RSCU, relative synonymous codon usage.

Introduction

The order Chiroptera is one of the most diverse groups of mammals, comprising more than 1,515 described species grouped into approximately 21 families [1]. Within this order, the family Phyllostomidae stands out for its high morphological and ecological diversity, as well as for the wide variety of trophic strategies exhibited by its species, including frugivory, nectarivory, insectivory, carnivory, and hematophagy [2, 3]. This diversity has made phyllostomids a group of particular interest for studying adaptation, diversification, and evolutionary processes in Neotropical bats.

Within Phyllostomidae, the genus *Artibeus* comprises approximately 23 species distributed from Mexico to South America and the Caribbean, representing one of the most diverse lineages in the family [2, 4]. Its members are generally characterized by a short rostrum, large, pointed ears, a well-developed noseleaf, pale facial stripes, brownish fur, and dark wing membranes [5]. Most species in the genus are predominantly frugivorous and play an important role in bat communities throughout Neotropical ecosystems.

Artibeus hirsutus, commonly known as the hairy fruit-eating bat, is a species endemic to Mexico, with its type locality in La Salada, Michoacán [6]. Among the larger-bodied species of the genus, *A. hirsutus* is one of the smaller species, with a forearm length ranging from 52.0 to 58.4 mm and an approximate body mass of 32.0 to 47.2 g [6, 7]. It is distinguished by its dense brown fur, grayish wing membranes, absence of a tail, and, particularly, the presence of a narrow uropatagium with a conspicuous fringe densely covered in hair, one of its most distinctive external characteristics [5, 6].

The distribution of *A. hirsutus* is restricted to Mexico and encompasses primarily the Pacific slope, from southern Sonora to Guerrero, extending into the lowlands of the Trans-Mexican Volcanic Belt and Morelos. The species has been recorded from areas near sea level to elevations of approximately 2,600 m [6, 7]. It is primarily associated with tropical deciduous forests, although it can also inhabit environments modified by human activities. Individuals have been documented in mango and fig orchards and in areas near bodies of water, while its daytime roosts include small caves, abandoned mines, buildings, and spaces beneath rocks [6, 7].

Available information on the population structure and reproduction of *A. hirsutus* remains relatively limited. Recent studies conducted in west-central Mexico indicate a pattern of bimodal seasonal polyestry, with two reproductive events throughout the year and birth periods occurring approximately in April and August [7]. These findings complement historical records of pregnant females between February and September and lactating females during June, August, and September [6]. Despite its relatively broad distribution across western Mexico, the species is generally found at low abundances and remains one of the least studied members of the genus in the country [7].

From a systematic perspective, *A. hirsutus* has historically been considered closely related to *A. inopinatus* based on morphological similarities. However, the two species can be distinguished by external and cranial characteristics, including the greater hair density on the uropatagium and larger body dimensions of *A. hirsutus* [6]. Subsequently, molecular analyses based on the mitochondrial cytochrome b gene recovered *A. hirsutus* as associated with *A. fraterculus*, whereas *A. inopinatus* was positioned as the sister group to that lineage; however, some of these interspecific relationships received limited support [8]. These differences between morphological and molecular approaches indicate that the internal relationships within *Artibeus* could benefit from the incorporation of additional genomic data.

Despite advances in the taxonomic, ecological, and reproductive knowledge of *A. hirsutus*, genomic information available for this species remains limited. The incorporation of complete mitochondrial genomes has made it possible to characterize patterns of gene organization, nucleotide composition, and phylogenetic relationships in different representatives of Phyllostomidae, providing a broad set of molecular characters for comparisons among species and lineages [3, 9]. In this context, characterization of the mitogenome of *A. hirsutus* represents an opportunity to expand the molecular representation available for the genus and assess its position within Phyllostomidae using a complete mitochondrial dataset.

Therefore, the present study aims to characterize the complete mitochondrial genome of *Artibeus hirsutus* through genome assembly and annotation, as well as to analyze its main genomic features, including nucleotide composition, relative synonymous codon usage, selective pressure on protein-coding genes, and the secondary structures of transfer RNA genes. In addition, the control region is examined, and the phylogenetic position of the species is assessed through a comparative analysis within Phyllostomidae. The generation of this information expands the genomic resources available for *Artibeus* and provides a molecular foundation for future studies on the systematics, evolution, and population genetics of Neotropical bats.

Materials and Methods

Sample Collection, DNA Extraction, and Sequencing

A wing membrane tissue sample of *Artibeus hirsutus* was obtained under scientific collection permit SGPNDGVS/00365/22 from El Salitre Cave, located in the state of Morelos, Mexico. The tissue was preserved in ethanol and stored at −80 °C until laboratory processing. Before extraction, the ethanol was removed by washing the sample twice with buffer under gentle agitation for 30 min, and excess liquid was removed using Kimtech Science paper.

The tissue was macerated with a sterile scalpel in a Petri dish containing PBS and subsequently centrifuged for 10 min at 10,000 × g. The supernatant was discarded, and the remaining material was incubated with 200 µL of ZymoBIOMICS lysis solution and 20 µL of proteinase K at 55 °C for 24 h. After centrifugation, the supernatant was recovered and treated with 10 µL of RNase for 5 min at 37 °C. Total DNA was extracted using the Quick-DNA HMW MagBead Kit (Cat. No. D6060), following the manufacturer's recommendations. The concentration of the extracted DNA was quantified using a NanoDrop 2000 spectrophotometer.

Shotgun genomic libraries with 150-bp paired-end reads were prepared and sequenced using Illumina sequencing-by-synthesis technology on a NovaSeq 6000 platform with an S4 flow cell. Subsequently, the mitogenome of A. hirsutus was assembled de novo using GetOrganelle software [10].

Mitochondrial Genome Assembly, Annotation, and Characterization

The mitogenome of *Artibeus hirsutus* was assembled *de novo* using GetOrganelle with a k-mer value of 115 [10]. The mitogenomes of *A. jamaicensis* and *A. lituratus*, available in GenBank under accession numbers NC_002009.1 and NC_016871.1, respectively, were used as references to guide the assembly.

Initial annotation of the assembled mitochondrial genome was performed using the MITOS and MITOS2 web servers with the vertebrate mitochondrial genetic code [11, 12]. The annotation was subsequently reviewed manually, including curation of protein-coding genes and verification of start and stop codons using the ExPASy Translate Tool [13]. A graphical representation of the mitogenome was generated using the GenomeVx web server [14].

The nucleotide composition of the mitogenome and ribosomal RNA genes was estimated using MEGA 11 [15]. Codon usage profiles of protein-coding genes were assessed using MEGA 11 and the Sequence Manipulation Suite tool [16]. In addition, relative synonymous codon usage values and amino acid frequencies were estimated to characterize codon usage bias patterns in the mitogenome of *A. hirsutus*.

The secondary structures of transfer RNA genes were predicted using the ViennaRNA/RNAfold web server [17]. Additionally, the control region was analyzed to identify microsatellites, tandem repeats, and potential hairpin secondary structures using the Sequence Manipulation Suite [16], the *in-silico* PCR and Microsatellite Repeats Finder server [18], Galaxy Europe-equicktandem, and RNAfold [17].

Selective Pressure Analysis

Selective pressure on the 13 mitochondrial protein-coding genes was assessed using the ratio of nonsynonymous to synonymous substitutions (Ka/Ks). For this purpose, the sequence of each protein-coding gene from *A. hirsutus* was aligned with its corresponding orthologous sequences from related Phyllostomidae species available in GenBank. Coding sequences were obtained from the annotations generated using MITOS2 [12], and Ka/Ks values were calculated using KaKs Calculator Toolbox 2.0 [19].

Phylogenetic Analysis

The phylogenetic position of *Artibeus hirsutus* within Phyllostomidae was assessed through a comparative analysis of the 13 mitochondrial protein-coding genes. The dataset included the mitogenome assembled in this study and the mitogenomes of 43 Phyllostomidae species available in GenBank. Two species representing other bat families were used as outgroups: *Myotis lucifugus* (Vespertilionidae) and *Molossus molossus* (Molossidae).

Protein-coding sequences were extracted using MitoPhAST [20]. Subsequently, nucleotide sequences were translated into amino acid sequences and aligned using Clustal Omega [21]. Regions with ambiguous or poor alignments were removed using trimAl [22]. The dataset was partitioned, and the most appropriate evolutionary models were selected using ProtTest [23]. Finally, phylogenetic inference was performed using the maximum-likelihood criterion with IQ-TREE [24], and the robustness of the resulting topology was assessed using 1,000 bootstrap replicates.

Results

Mitochondrial Genome Assembly and Organization

The complete mitochondrial genome of *Artibeus hirsutus* (GenBank: PP853570.1) was 16,670 bp long and comprised the 37 genes characteristic of vertebrate mitogenomes: 13 protein-coding genes (PCGs), 22 transfer RNA genes (tRNAs), and two ribosomal RNA genes (rRNAs), in addition to a non-coding control region (Figure 1; Table 1). Most genes were encoded on the heavy strand (H). The light strand (L) contained the nad6 gene and eight tRNA genes: *trnQ, trnA, trnN, trnC, trnY, trnS2, trnE*, and *trnP* (Table 1). Among the PCGs, *cox1*, *nad5*, and *cob* were among the longest genes, whereas *atp8* was one of the shortest genes.

Thirteen overlapping regions were identified in the mitogenome: nine short overlaps of 1–3 bp and four longer overlaps of 7, 9, 17, and 43 bp. The largest overlap occurred between the *atp8* and *atp6* genes, spanning 43 bp. The 13 PCGs used only two start codons: ten genes used ATG, whereas three used ATA (Table 1). Regarding stop codons, nine genes contained TAA, *nad2* used TAG, and *cob* terminated with AGA. The *cox3* and *nad4* genes had an incomplete stop codon, T.

Nucleotide Composition and Codon Usage

The nucleotide composition of the complete mitochondrial genome of *A. hirsutus* was A = 32.4%, T = 29.5%, C = 24.9%, and G = 12.99%, with a total A+T content of 62.03% and a C+G content of 37.9%. The ribosomal genes 12S and 16S were located in the region between trnF and trnL2, separated by trnV. The 16S gene, approximately 1,560 bp long, exhibited a nucleotide composition of T = 25.6%, C = 20.3%, A = 36.9%, and G = 17.05%, with an A+T content of 62.56%. In contrast, the 12S gene, approximately 971 bp long, exhibited T = 24.3%, C = 23.6%, A = 33.77%, and G = 18.22%, with an A+T content of 58.08%.

Analysis of codon usage in the PCGs revealed a marked preference for certain A- and T-rich codons (Table 2; Figure 2). The most frequent codons were CTA (Leu), with 265 occurrences and a frequency of 69.61 per 1,000 codons; ATA (Met), with 211 occurrences and a frequency of 55.42 per 1,000 codons; and ATT (Ile), with 205 occurrences and a frequency of 53.85 per 1,000 codons. In contrast, the least represented codons were TGG (Trp) and CAG (Gln), each used only once; CGG (Arg), with two occurrences; and CCG (Pro), with four occurrences.

Selective Pressure

Analysis of the ratio of nonsynonymous to synonymous substitutions (Ka/Ks; ω) across the 13 PCGs revealed values below 1 in all comparisons performed (Figure 3). The mean Ka/Ks ratio was 0.0371 ± 0.0738. Among the genes analyzed, *atp8* exhibited the highest Ka/Ks values in both comparisons, with a particularly high value in the comparison between *A. hirsutus* and *Leptonycteris yerbabuenae*. In contrast, *cox1*, *cox2*, and *cox3* exhibited some of the lowest values. Complex I genes (*nad1–nad6* and *nad4L*) showed intermediate values that varied among the comparisons performed.

Secondary Structure of tRNAs

Most of the 22 tRNA genes of *A. hirsutus* exhibited the classical cloverleaf secondary structure, consisting of the acceptor arm, DHU arm, anticodon arm, and TΨC arm (Figure 4). The main exception was *trnS1*, which lacks the DHU arm.

Control Region

The control region (CR) was 1,238 bp long and was located between *trnP* and *trnF* in the circular genome (Figure 1). Nine period-2 repetitive regions were identified within the control region, each consisting of three repeat units and having a minimum length of 6 bp. These regions were predominantly enriched in A and T,

although repeats with higher G and C content were also identified. The control region also exhibited hairpin-like secondary structures. Thermodynamic analysis revealed an ensemble free energy of −295.65 kcal/mol, an ensemble diversity of 321.97, and a frequency of the minimum free energy structure of 0.00%. The centroid structure had an energy of −172.10 kcal/mol. These values correspond to distinct properties of the predicted structural ensemble and do not represent a single estimate of minimum energy.

A tandem repeat with a period of 14 bp was also detected, located between positions 763 and 939 of the control region and repeated approximately 12.6 times. The copies exhibited approximately 96% similarity, with a nucleotide composition of C = 45%, A = 29%, G = 19%, and T = 6%.

Phylogenetic Analysis

Maximum-likelihood phylogenetic analysis based on the concatenated alignment of the 13 mitochondrial PCGs placed *Artibeus hirsutus* within the clade corresponding to Stenodermatinae, where it clustered with other representatives of the genus *Artibeus*, including *A. jamaicensis* and *A. lituratus* (Figure 5). The tree also recovered clusters corresponding to different subfamilies of Phyllostomidae, including Stenodermatinae, Carolliinae, Glossophaginae, Phyllostominae, Lonchorhininae, Lonchophyllinae, and Desmodontinae, as well as other lineages represented in the sampling. *Myotis lucifugus* (Vespertilionidae) and *Molossus molossus* (Molossidae) were used as outgroups to root the tree. Representatives of Desmodontinae were recovered as a distinct internal lineage within Phyllostomidae.

Discussion

Mitogenome Organization and Composition

The mitogenome length of 16,670 bp obtained for *A. hirsutus* is comparable to that reported for other representatives of Phyllostomidae, such as *Artibeus jamaicensis* (16,651 bp), *A. lituratus* (16,709 bp), *Ectophylla alba* (16,664 bp), *Macrotus waterhousii* (16,792 bp), and *M. californicus* (16,691 bp) [25–28]. These similarities reflect the general conservation of mitochondrial architecture within Phyllostomidae, despite minor variations in total genome length among species.

The distribution of genes between the heavy (H) and light (L) strands is consistent with the pattern previously described for other phyllostomids and mammals, in which nad6 and a small set of tRNA genes are encoded on the light strand. This arrangement indicates a high degree of conservation of mitochondrial synteny within Chiroptera [9, 25, 28, 29]. Similarly, the presence of overlapping regions, including the 43-bp overlap between *atp8* and *atp6*, falls within the structural patterns observed in mammalian mitogenomes. Despite these overlapping regions, the overall gene order of *A. hirsutus* remains conserved relative to that of other representatives of Phyllostomidae.

The presence of incomplete stop codons in *cox3* and *nad4* is also a well-documented feature of mitochondrial DNA in mammals and other bats. These codons may be completed during post-transcriptional processing through polyadenylation [12, 30, 31]. The A+T content of 62.03% observed in *A. hirsutus* is consistent with the nucleotide bias described for other phyllostomids. *A. jamaicensis* exhibits approximately

62% A+T, whereas *E. alba* has been reported to exhibit a nucleotide composition of A = 33.4%, T = 28.8%, C = 24.7%, and G = 13.0%, with a total A+T content of 62.2% [25, 27]. A similar pattern has also been documented in *M. waterhousii* and *M. californicus* [28].

The low proportion of guanine observed in *A. hirsutus* is part of the compositional bias characteristic of mammalian mitochondrial DNA. This pattern has been associated with asymmetric mutation processes linked to mitochondrial DNA (mtDNA) replication, during which the two strands remain exposed under different conditions and for different periods, favoring differential substitution rates [32]. Furthermore, the presence of independent replication origins for each strand contributes to the characteristic nucleotide biases observed in vertebrate mitogenomes [33]. The 12S and 16S genes also retained an A+T predominance, consistent with the overall pattern observed in the mitogenome.

Codon Usage and Selective Pressure

The high representation of leucine, isoleucine, and methionine, together with the general preference for A- and T-rich codons, is consistent with the compositional bias of the *A. hirsutus* mitogenome. Similar patterns have been described in *A. jamaicensis*, *E. alba*, *Macrotus* spp., and other bats, suggesting a close relationship between nucleotide composition and codon usage in mitochondrial genes [25–28].

Likewise, the distribution of PCG lengths agrees with observations in other phyllostomids, in which *cox1*, *nad5*, and *cob* are among the longest genes, whereas *atp8* is among the shortest. This pattern has been documented in *E. alba*, *Macrotus* spp., and representatives of *Leptonycteris* [27, 28, 31].

The Ka/Ks values below 1 obtained for all 13 PCGs indicate a predominance of purifying selection acting on mitochondrial protein-coding genes. This pattern is consistent with findings reported for Phyllostomidae, Vespertilionidae, Rhinolophidae, and Pteropodidae, in which mitochondrial PCGs are primarily subject to purifying selection because of their direct involvement in oxidative phosphorylation and cellular energy production [9, 26–28, 31].

Although *atp8* exhibited the highest Ka/Ks values in both comparisons, these values remained below 1. Therefore, this pattern does not constitute evidence of positive selection but rather indicates relatively weaker evolutionary constraint on *atp8* compared with other PCGs, as well as a comparatively higher rate of nonsynonymous substitutions within an overall context of purifying selection. The particularly pronounced difference in the comparison with *L. yerbabuenae* could be associated, among other factors, with the greater phylogenetic divergence between the taxa compared.

In contrast, *cox1*, *cox2*, and *cox3* exhibited some of the lowest Ka/Ks values, indicating a high degree of evolutionary conservation. These genes encode essential components of complex IV of the mitochondrial respiratory chain; therefore, potentially deleterious amino acid changes are subject to strong purifying selection. Similar conservation of cox genes has previously been documented in other bats [26, 27]. Complex I genes (*nad1–nad6* and *nad4L*) exhibited intermediate and variable values, indicating that the relative

strength of evolutionary constraint is not uniform across the different components of the oxidative phosphorylation (OXPHOS) system.

Secondary Structure of tRNAs

The cloverleaf structure observed in most tRNAs of A. hirsutus is consistent with the general pattern described for other phyllostomids. The absence of the DHU arm in trnS1 is not unique to this species, as it has also been documented in *E. alba*, *M. waterhousii*, and *M. californicus* [27, 28]. Likewise, a high degree of conservation in tRNA secondary structures has previously been described in *A. jamaicensis* [25].

The absence of the DHU arm in tRNA-Ser1 is a recurrent modification in metazoan mitogenomes and does not necessarily imply a loss of tRNA functionality, as this molecule may retain its capacity for recognition and participation in translation through compensatory structural interactions [28, 29, 34, 35]. In this regard, the organization observed in *A. hirsutus* reflects both a high degree of structural conservation and the presence of recurrent secondary modifications in animal mitochondrial DNA.

Control Region

The control region of *A. hirsutus*, measuring 1,238 bp, is comparable in length to those reported for *A. jamaicensis* (1,229 bp), *E. alba* (1,232 bp), and *M. californicus* (1,232 bp), although it is shorter than that described for *M. waterhousii* (1,336 bp) [25, 27, 28]. These differences suggest that variation in control region length contributes to the differences observed in the overall size of phyllostomid mitogenomes.

The presence of microsatellites and other repetitive sequences is a common feature of the mitochondrial control region, whose rate of structural change is generally higher than that observed in coding regions [25, 27, 28, 31]. In *A. hirsutus*, the presence of nine repetitive regions and a 14-bp tandem repeat comprising approximately 12.6 copies indicates considerable structural heterogeneity within this region. This repetitive arrangement could contribute to the length variation observed among species and even among haplotypes within the same lineage.

Hairpin structures have also been described in the control region of *A. jamaicensis*, where secondary elements consisting of stems and loops were identified [25]. In other phyllostomids, such as *E. alba*, *Macrotus* spp., and *Leptonycteris* spp., conserved functional domains and repetitive sequences have also been documented in this region [27, 28, 31]. The coexistence of tandem repeats, microsatellites, and secondary structures confirms that the control region is one of the most structurally variable portions of the *A. hirsutus* mitogenome. Given this variability, these elements could be evaluated in future studies as markers for population genetics, phylogeography, and intraspecific variation, although their utility must be validated through targeted population sampling.

Phylogenetic Position and Evolutionary Context

The placement of *A. hirsutus* within Stenodermatinae and its association with other representatives of the genus *Artibeus* are consistent with previous phylogenetic studies that recognize this genus as a stenodermatine

lineage within Phyllostomidae [2, 3, 9, 25]. The recovered position of *A. hirsutus* is also consistent with the ecological diversity characteristic of Stenodermatinae, a subfamily that includes numerous predominantly frugivorous taxa, such as *Artibeus*, *Sturnira*, and *Platyrrhinus* [2, 28, 36, 37]. In contrast, Phyllostomidae includes lineages with markedly different trophic strategies, including insectivory, nectarivory, omnivory, and hematophagy, reflecting extensive ecological radiation within the family.

Some lineages, such as Micronycterinae and Lonchorhininae, were recovered in early-diverging positions within the topology, whereas Stenodermatinae comprises clades primarily associated with frugivory. This distribution is consistent with previous hypotheses regarding the evolution of feeding strategies in Phyllostomidae. However, the relationship between diet and diversification should not be interpreted as a linear transition, since different trophic habits have arisen through complex processes of specialization and adaptive convergence [3]. Furthermore, the resulting topology makes it possible to establish phylogenetic relationships among the included taxa but does not, by itself, provide a temporal estimate of divergence events.

Conclusion

Characterization of the complete mitochondrial genome of *Artibeus hirsutus* revealed a conserved organization relative to other representatives of Phyllostomidae, in terms of gene number and arrangement, nucleotide composition, and overall structure. The protein-coding genes exhibited Ka/Ks values below 1, indicating a predominance of purifying selection, whereas *atp8* showed relatively weaker evolutionary constraint compared with other mitochondrial genes. Most tRNAs retained the typical cloverleaf secondary structure, with the exception of trnS1, which lacked the DHU arm. The control region contained microsatellites, tandem repeats, and secondary structures, indicating greater structural variability relative to coding regions. Finally, phylogenetic analysis placed *A. hirsutus* within Stenodermatinae, associated with other representatives of *Artibeus*. Collectively, these results expand the genomic information available for this species and provide a foundation for future comparative, phylogenetic, and population-level studies within Phyllostomidae.

Declarations and Statements

Funding

This work was conducted as part of a multidisciplinary project led by Dr. Jorge Ortega, focused on the sequencing and characterization of mitogenomes from different bats in Mexico (Proyecto Ciencia de Frontera 15307). The project received partial support from the Secretaría de Investigación y Posgrado – Instituto Politécnico Nacional within the framework of this multidisciplinary project (PM 02-2355 and 20260163).

Conflicts of Interest

The authors declare that they have no financial or non-financial interests related to the work presented.

Authors' Contributions

María Fernanda Cruz Díaz conducted the original research as part of her thesis, performed the laboratory procedures, and carried out the bioinformatic analyses. **Carlos F. Calderón-Palapa** contributed bioinformatic support, interpretation of the analyses, and the preparation and structuring of the manuscript, from its initial draft based on the thesis work. **Jorge Ortega** contributed to funding acquisition, field sample collection, and overall project supervision. All authors reviewed and approved the final version of the manuscript.

Ethical Approval

The biological material used in this study was obtained under a scientific collection permit issued by the General Directorate of Wildlife (Dirección General de Vida Silvestre) of the Secretariat of Environment and Natural Resources (Secretaría de Medio Ambiente y Recursos Naturales, SEMARNAT), Mexico, under official authorization No. SGPNDGVS/00365/22. The authorization covers the research area entitled "Ecology and Conservation Genetics of Mammals for Understanding National Biodiversity" and the project "Population Genetics of Mexican Bats." The permit authorizes the capture of specimens belonging to the order Chiroptera, the collection of wing membrane tissue samples for genetic analyses, and the subsequent release of specimens at the collection site, in accordance with applicable Mexican regulations.

References

1. Simmons NB, Cirranello AL (2025) Bat species of the world: A taxonomic and geographic database. American Museum of Natural History. https://batnames.org/. Accessed October 13, 2026
2. Baker RJ, Hoofer SR, Porter CA, Van Den Bussche RA (2003) Diversification among New World leaf-nosed bats: An evolutionary hypothesis and classification inferred from digenomic congruence of DNA sequence. Occasional Papers, Museum of Texas Tech University 230:1–32. https://doi.org/10.5962/bhl.title.142891
3. Camacho A, Cadar D, Horváth B, Merino-Viteri A, Murienne J (2022) Revised phylogeny from complete mitochondrial genomes of phyllostomid bats resolves subfamilial classification. Zoological Journal of the Linnean Society 196:1591–1607. https://doi.org/10.1093/zoolinnean/zlac055
4. Van Den Bussche RA, Baker RJ (1993) Molecular phylogenetics of Phyllostomidae. Journal of Mammalogy 74:735–747.
5. Tuttle MD (2019) Bats: An illustrated guide to all species. Ivy Press.
6. Webster WD, Jones JK Jr (1983) *Artibeus hirsutus*. Mammalian Species 199:1–3.
7. Zalapa S, García-Sandoval R, Guerrero-Vázquez S, Pérez-Arteaga A, Romero-Almaraz M, Sánchez-Hernández C (2023) Population structure and reproduction of the hairy fruit-eating bat, *Artibeus hirsutus*, in central-western México. Revista Mexicana de Biodiversidad 94:e945127. https://doi.org/10.22201/ib.20078706e.2023.94.5127
8. Lim BK, Engstrom MD, Lee TE Jr, Patton JC, Bickham JW (2004) Molecular differentiation of large species of fruit-eating bats (*Artibeus*) and phylogenetic relationships based on the cytochrome b gene. Acta Chiropterologica 6:1–12.

9. Botero-Castro F, Tilak M, Justy F, Catzeflis F, Delsuc F, Douzery EJP (2013) Next-generation sequencing and phylogenetic signal of complete mitochondrial genomes for resolving the evolutionary history of leaf-nosed bats (Phyllostomidae). Molecular Phylogenetics and Evolution 69:728–739. https://doi.org/10.1016/j.ympev.2013.07.003

10. Jin J, Yu W, Yang J, Song Y, de Pamphilis CW, Yi T, Li D (2020) GetOrganelle: a fast and versatile toolkit for accurate de novo assembly of organelle genomes. Genome Biology 21:241. https://doi.org/10.1186/s13059-020-02154-5

11. Bernt M, Donath A, Jühling F, Externbrink F, Florentz C, Fritzsch G, Pütz J, Middendorf M, Stadler PF (2013) MITOS: Improved *de novo* metazoan mitochondrial genome annotation. Molecular Phylogenetics and Evolution 69:313–319. https://doi.org/10.1016/j.ympev.2012.08.023

12. Donath A, Jühling F, Al-Arab M, Bernhart SH, Reinhardt F, Stadler PF, Middendorf M, Bernt M (2019) Improved annotation of protein-coding gene boundaries in metazoan mitochondrial genomes. Nucleic Acids Research 47:10543–10552. https://doi.org/10.1093/nar/gkz833

13. Gasteiger E, Gattiker A, Hoogland C, Ivanyi I, Appel RD, Bairoch A (2003) ExPASy: The proteomics server for in-depth protein knowledge and analysis. Nucleic Acids Research 31:3784–3788. https://doi.org/10.1093/nar/gkg563

14. Conant GC, Wolfe KH (2008) GenomeVx: simple web-based creation of editable circular chromosome maps. Bioinformatics 24:861–862. https://doi.org/10.1093/bioinformatics/btm598

15. Tamura K, Stecher G, Kumar S (2021) MEGA11: Molecular Evolutionary Genetics Analysis version 11. Molecular Biology and Evolution 38:3022–3027. https://doi.org/10.1093/molbev/msab120

16. Stothard P (2000) The sequence manipulation suite: JavaScript programs for analyzing and formatting protein and DNA sequences. BioTechniques 28:1102–1104. https://doi.org/10.2144/00286ir01

17. Gruber AR, Lorenz R, Bernhart SH, Neuböck R, Hofacker IL (2008) The Vienna RNA Website. Nucleic Acids Research 36:W70–W74. https://doi.org/10.1093/nar/gkn188

18. Bikandi J, Millán RS, Rementeria A, Garaizar J (2004) *In silico* analysis of complete bacterial genomes: PCR, AFLP-PCR and endonuclease restriction. Bioinformatics 20:798–799. https://doi.org/10.1093/bioinformatics/btg491

19. Wang D, Zhang Y, Zhang Z, Zhu J, Yu J (2010) KaKs_Calculator 2.0: A toolkit incorporating gamma-series methods and sliding window strategies. Genomics, Proteomics & Bioinformatics 8:77–80. https://doi.org/10.1016/S1672-0229(10)60008-3

20. Tan MH, Gan HM, Schultz MB, Austin CM (2015) MitoPhAST, a new automated mitogenomic phylogeny tool in the post-genomic era. Mitochondrial DNA 26:643–647.

21. Sievers F, Higgins DG (2014) Clustal Omega. Current Protocols in Bioinformatics 48:3.13.1–3.13.16. https://doi.org/10.1002/0471250953.bi0313s48

22. Capella-Gutiérrez S, Silla-Martínez JM, Gabaldón T (2009) trimAl: A tool for automated alignment trimming in large-scale phylogenetic analyses. Bioinformatics 25:1972–1973. https://doi.org/10.1093/bioinformatics/btp348

23. Abascal F, Zardoya R, Posada D (2005) ProtTest: Selection of best-fit models of protein evolution. Bioinformatics 21:2104–2105. https://doi.org/10.1093/bioinformatics/bti263

24. Nguyen LT, Schmidt HA, von Haeseler A, Minh BQ (2015) IQ-TREE: a fast and effective stochastic algorithm for estimating maximum-likelihood phylogenies. Molecular Biology and Evolution 32:268–274. https://doi.org/10.1093/molbev/msu300

25. Pumo DE, Finamore PS, Franek WR, Phillips CJ, Tarzami S, Balzarano D (1998) Complete mitochondrial genome of a neotropical fruit bat, *Artibeus jamaicensis*, and a new hypothesis of the relationships of bats to other eutherian mammals. Journal of Molecular Evolution 47:709–717.

26. Meganathan PR, Pagan HJT, McCulloch ES, Stevens RD, Ray DA (2012) Complete mitochondrial genome sequences of three bat species and whole genome mitochondrial analyses reveal patterns of codon bias and lend support to a basal split in Chiroptera. Gene 492:121–129.

27. Vivas-Toro I, Ortega J, Baeza JA (2021) The complete mitochondrial genome of the Honduran white bat *Ectophylla alba* (Allen 1982) (Chiroptera: Phyllostomidae). Gene 802:145868. https://doi.org/10.1016/j.gene.2021.145868

28. Vargas-Trejo KJ, Ortega J, Gutiérrez-Guerrero YT, Gutiérrez EG, Baeza JA (2023) The mitochondrial genomes of big-eared bats, *Macrotus waterhousii* and *Macrotus californicus* (Chiroptera: Phyllostomidae: Macrotinae). Gene 863:147295. https://doi.org/10.1016/j.gene.2023.147295

29. Molina M, Oliveira G, Oliveira R, Nunes G, Pires E, Prous X, Ribeiro M, Vasconcelos S (2024) Complete mitochondrial genomes of cave bats and their phylogenetic relationships. PLoS ONE 19:e0308741. https://doi.org/10.1371/journal.pone.0308741

30. Taanman JW (1999) The mitochondrial genome: structure, transcription, translation and replication. Biochimica et Biophysica Acta (BBA) - Bioenergetics 1410:103–123. https://doi.org/10.1016/S0005-2728(98)00161-3

31. Barrera CA, Ortega J, Gutiérrez-Guerrero YT, Baeza JA (2023) Comparative mitochondrial genomics of American nectar-feeding long-nosed bats *Leptonycteris* spp. with insights into the phylogeny of the family Phyllostomidae. Gene 879:147588. https://doi.org/10.1016/j.gene.2023.147588

32. Hassanin A, Léger N, Deutsch J (2005) Evidence for multiple reversals of asymmetric mutational constraints during the evolution of the mitochondrial genome of metazoa, and consequences for phylogenetic inferences. Systematic Biology 54:277–298. https://doi.org/10.1080/10635150590947843

33. Sahyoun AH, Duret L, Galtier N (2014) Life history determinants of the direction of mitochondrial DNA replication in metazoa. Molecular Biology and Evolution 31:383–393.

34. de Bruijn MHL, Schreier PH, Eperon IC, Barrell BG, Chen EY, Armstrong PW, Wong JFH, Roe BA (1980) A mammalian mitochondrial serine transfer RNA lacking the “dihydrouridine” loop and stem. Nucleic Acids Research 8:5213–5222. https://doi.org/10.1093/nar/8.22.5213

35. Jühling F, Pütz J, Florentz C, Stadler PF (2012) Improved systematic tRNA gene annotation allows new insights into the evolution of mitochondrial tRNA structures and into the mechanisms of mitochondrial genome rearrangements. PLoS ONE 7:e35061. https://doi.org/10.1371/journal.pone.0035061

36. Dávalos LM, Cirranello AL, Geisler JH, Simmons NB (2012) Understanding phylogenetic incongruence: Lessons from phyllostomid bats. Biological Reviews 87:991–1024. https://doi.org/10.1111/j.1469-185X.2012.00220.x

37. Dávalos LM, Velazco PM, Warsi OM, Smits PD, Simmons NB (2014) Integrating incomplete fossils by isolating conflicting signal in saturated and non-independent morphological characters. Systematic Biology 63:582–600. https://doi.org/10.1093/sysbio/syu013

Figures and Tables

Table 1. Annotation and structural organization of the mitochondrial genome of *Artibeus hirsutus*. CR: control region.

Name	Type	Start	Stop	Strand	Size (pb)	Start codon	Stop codon	Anti-codon	Continuity
trnF(gaa)	tRNA	1	71	+	70				-1
rrnS	rRNA	71	1040	+	970				1
trnV(tac)	tRNA	1042	1111	+	70				0
rrnL	rRNA	1112	2671	+	1559				1
trnL2(taa)	tRNA	2673	2747	+	74				2
nad1	Coding	2750	3706	+	956	ATG	TAA		-1
trnI(gat)	tRNA	3706	3774	+	69				-3
trnQ(ttg)	tRNA	3772	3844	-	73				-1
trnM(cat)	tRNA	3844	3912	+	69				0
nad2	Coding	3913	4956	+	1044	ATA	TAG		-2
trnW(tca)	tRNA	4955	5022	+	68				7
trnA(tgc)	tRNA	5029	5097	-	69				1
trnN(gtt)	tRNA	5099	5171	-	73				33
trnC(gca)	tRNA	5205	5270	-	66				0
trnY(gta)	tRNA	5271	5335	-	65				1
cox1	Coding	5337	6881	+	1545	ATG	TAA		-3
trnS2(tga)	tRNA	6879	6947	-	69				6
trnD(gtc)	tRNA	6954	7020	+	67				0
cox2	Coding	7021	7704	+	684	ATG	TAA		3
trnK(ttt)	tRNA	7708	7776	+	68				0
atp8	Coding	7777	7980	+	204	ATG	TAA		-43
atp6	Coding	7938	8618	+	681	ATG	TAA		-1
cox3	Coding	8618	9401	+	784	ATG	T		0
trnG(tcc)	tRNA	9402	9470	+	69				-3
nad3	Coding	9468	9818	+	351	ATA	TAA		0

trnR(tcg)	tRNA	9819	9886	+	68			0
nad4l	Coding	9887	10183	+	297	ATG	TAA	-7
nad4	Coding	10177	11554	+	1378	ATG	T	0
trnH(gtg)	tRNA	11555	11623	+	69			0
trnS1(gct)	tRNA	11624	11682	+	59			1
trnL (tag)	tRNA	11684	11753	+	70			-9
nad5	Coding	11745	13574	+	1830	ATA	TAA	-17
nad6	Coding	13558	14085	-	528	ATG	TAA	0
trnE(ttc)	tRNA	14086	14153	-	68			4
cob	Coding	14158	15297	+	1140	ATG	AGA	0
trnT(tgt)	tRNA	15298	15364	+	67			-1
trnP(tgg)	tRNA	15364	15431	-	68			
CR		15432	16670	+	1238			

Table 2. Codon usage in the mitochondrial protein-coding genes of *Artibeus hirsutus*. For each codon, the total number of occurrences (Count), frequency per 1,000 codons, and relative fraction are presented.

Ala	GCG	6	1.58	0.03
	GCA	79	20.75	0.33
	GCT	77	20.23	0.32
	GCC	77	20.23	0.32
Cys	TGT	9	2.36	0.38
	TGC	15	3.94	0.63
Asp	GAT	37	9.72	0.56
	GAC	29	7.62	0.44
Glu	GAG	10	2.63	0.11
	GAA	82	21.54	0.89
Phe	TTT	122	32.05	0.55
	TTC	101	26.53	0.45
Gly	GGG	18	4.73	0.08
	GGA	94	24.69	0.43
	GGT	47	12.35	0.22
	GGC	58	15.24	0.27
His	CAT	50	13.13	0.52
	CAC	47	12.35	0.48
Ile	ATT	205	53.85	0.63
	ATC	120	31.52	0.37
Lys	AAG	8	2.1	0.09
	AAA	85	22.33	0.91
Leu	TTG	11	2.89	0.02
	TTA	134	35.2	0.21
	CTG	14	3.68	0.02
	CTA	265	69.61	0.42
	CTT	110	28.89	0.18
	CTC	92	24.17	0.15
Met	ATG	32	8.41	0.13
	ATA	211	55.42	0.87
Asn	AAT	81	21.28	0.55
	AAC	65	17.07	0.45
Pro	CCG	4	1.05	0.02
	CCA	78	20.49	0.4
	CCT	51	13.4	0.26
	CCC	62	16.29	0.32
Gln	CAG	1	0.26	0.01
	CAA	82	21.54	0.99
Arg	CGG	2	0.53	0.03
	CGA	38	9.98	0.57
	CGT	10	2.63	0.15
	CGC	17	4.47	0.25
Ser	AGT	23	6.04	0.08
	AGC	33	8.67	0.12
	TCG	4	1.05	0.01
	TCA	88	23.12	0.31
	TCT	81	21.28	0.29
	TCC	55	14.45	0.19
Thr	ACG	8	2.1	0.02
	ACA	136	35.72	0.4
	ACT	107	28.11	0.31
	ACC	92	24.17	0.27
Val	GTG	12	3.15	0.06
	GTA	97	25.48	0.52
	GTT	47	12.35	0.25
	GTC	32	8.41	0.17
Trp	TGG	1	0.26	0.01
	TGA	104	27.32	0.99
Tyr	TAT	87	22.85	0.62
	TAC	53	13.92	0.38
End	AGG	0	0	0
	AGA	1	0.26	0.09
	TAG	1	0.26	0.09
	TAA	9	2.36	0.82

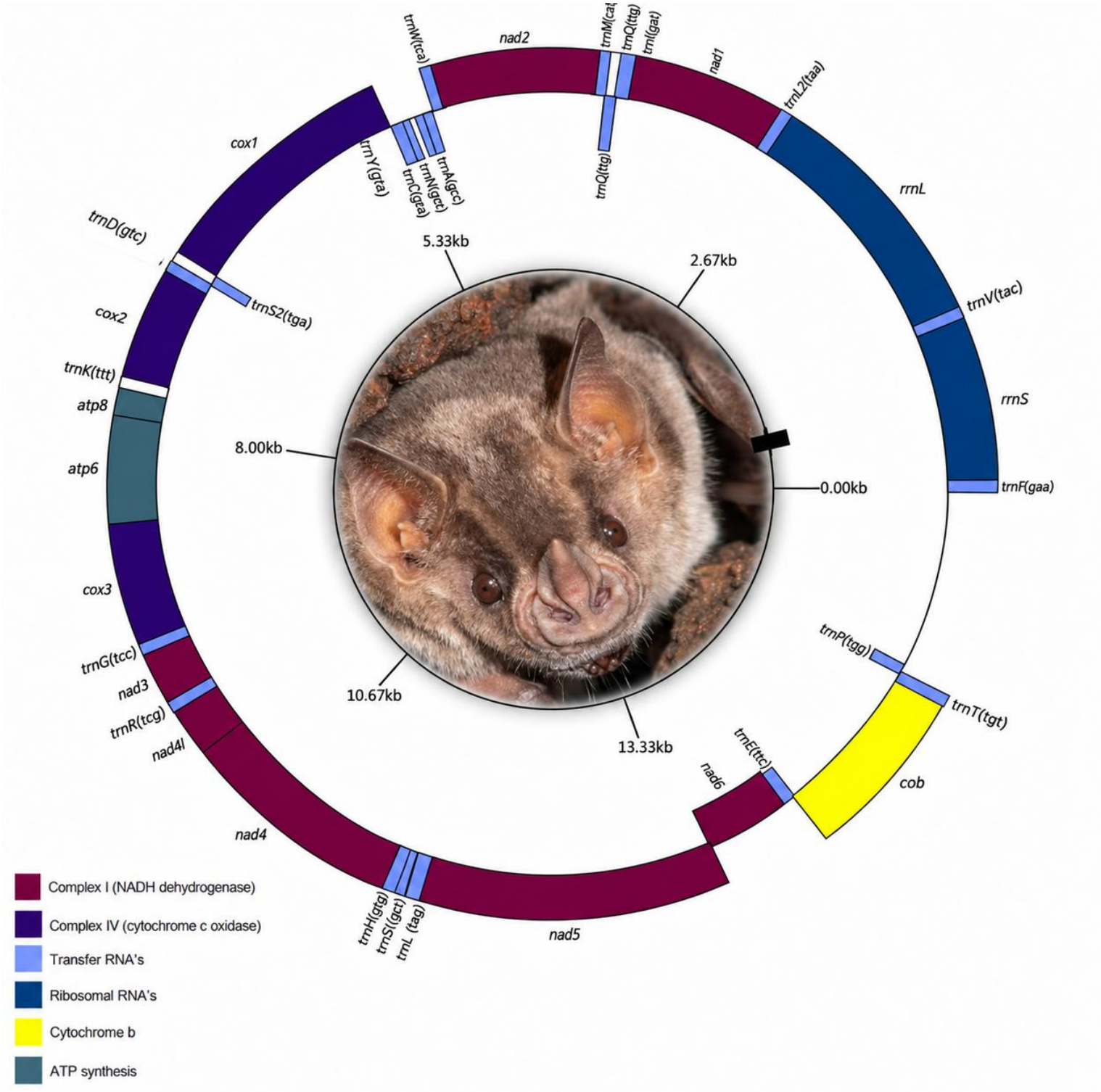


Fig. 1 Circular map of the mitochondrial genome of *Artibeus hirsutus*. The map shows the annotation of the 13 protein-coding genes (PCGs), two ribosomal RNA genes, 22 transfer RNA genes, and the putative control region. Genes encoded on the heavy strand are displayed toward the outer ring, whereas genes encoded on the light strand are shown toward the inner ring. Photograph of *Artibeus hirsutus* by José G. Martínez-Fonseca.

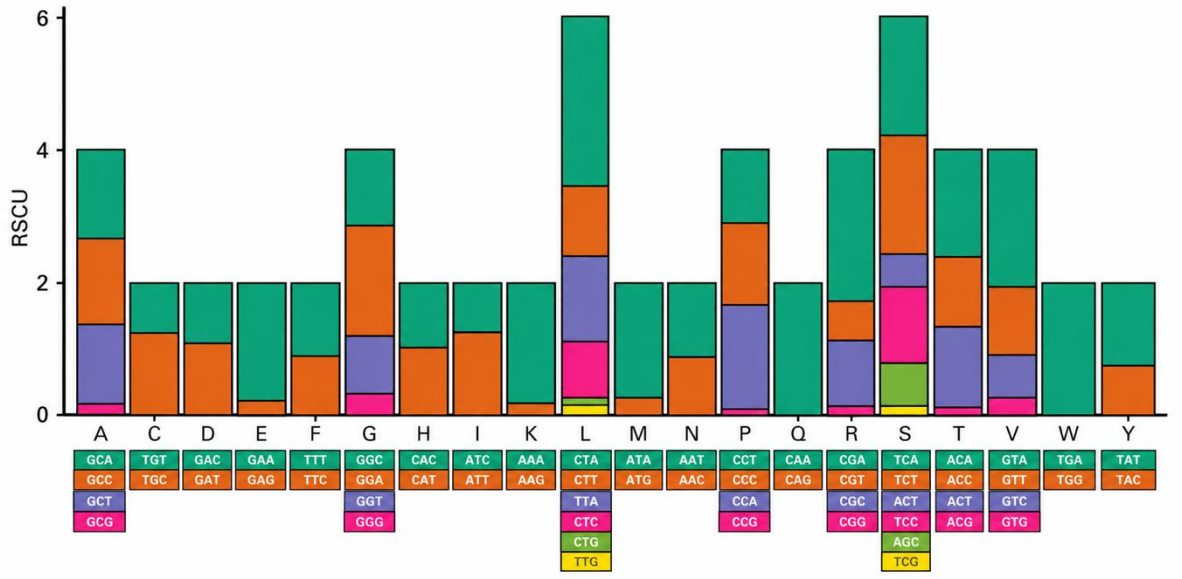


Fig. 2 Relative synonymous codon usage (RSCU) of the PCGs of *Artibeus hirsutus*.

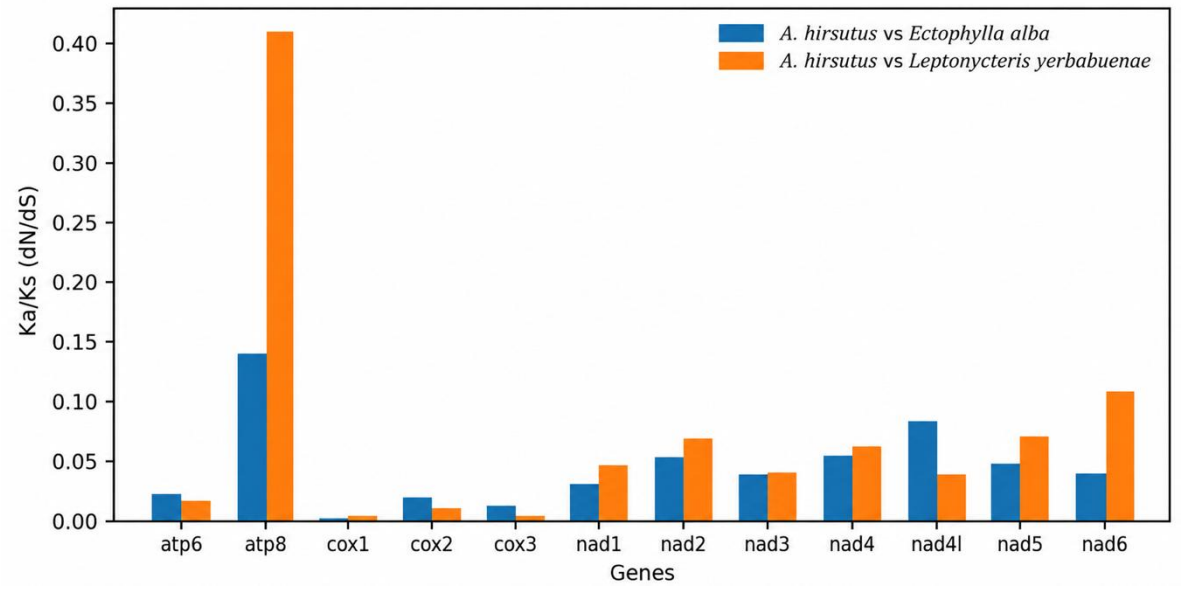


Fig. 3 Ka/Ks ratios of the PCGs of *Artibeus hirsutus* compared with *Ectophylla alba* and *Leptonycteris yerbabuenae*.

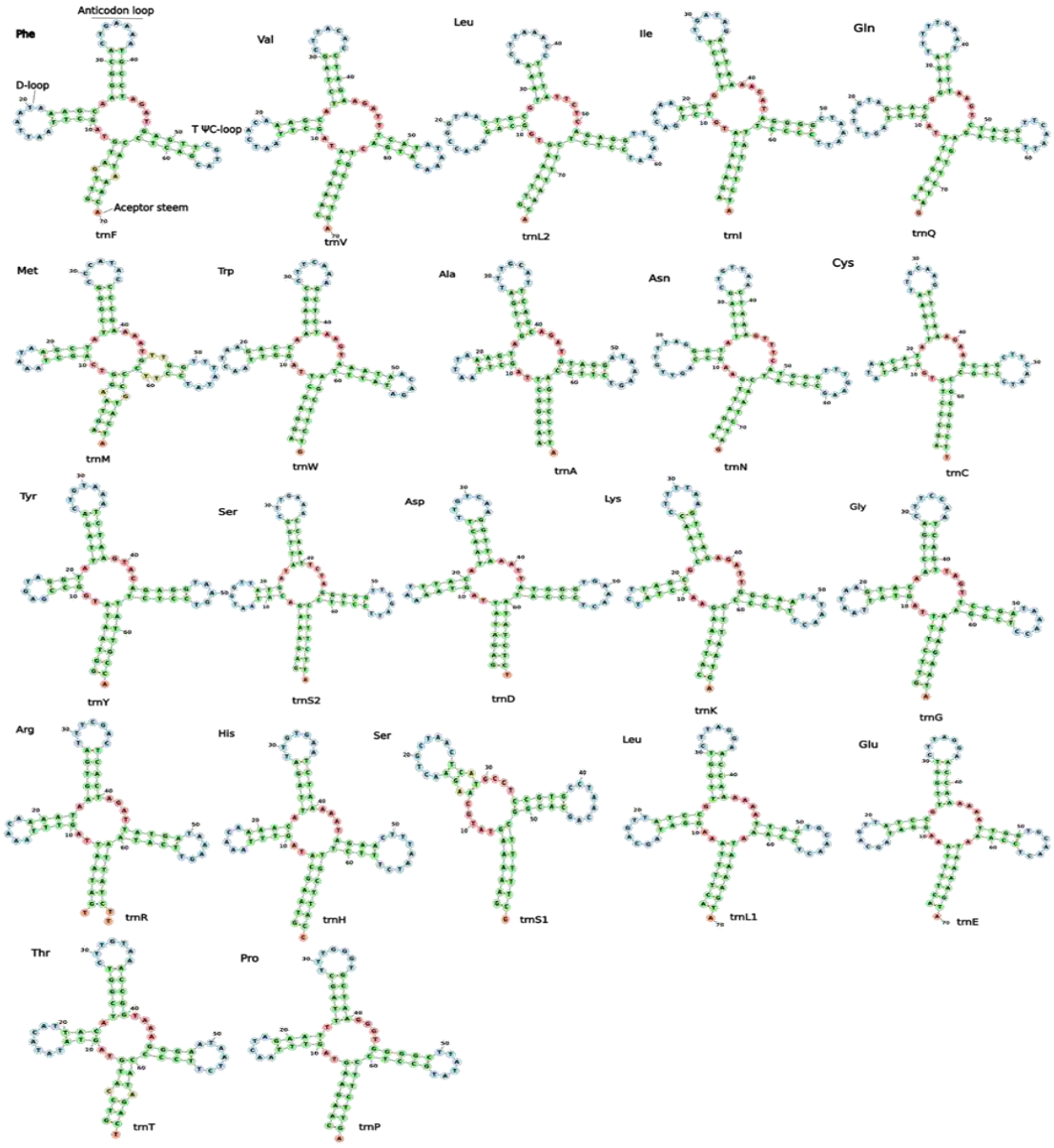


Fig. 4 Secondary structures of the 22 tRNAs in the mitochondrial genome of *Artibeus hirsutus*. Most tRNAs exhibit the typical cloverleaf structure; *trnS1* is the exception, lacking the DHU arm. Secondary structures were predicted using the ViennaRNA web server.

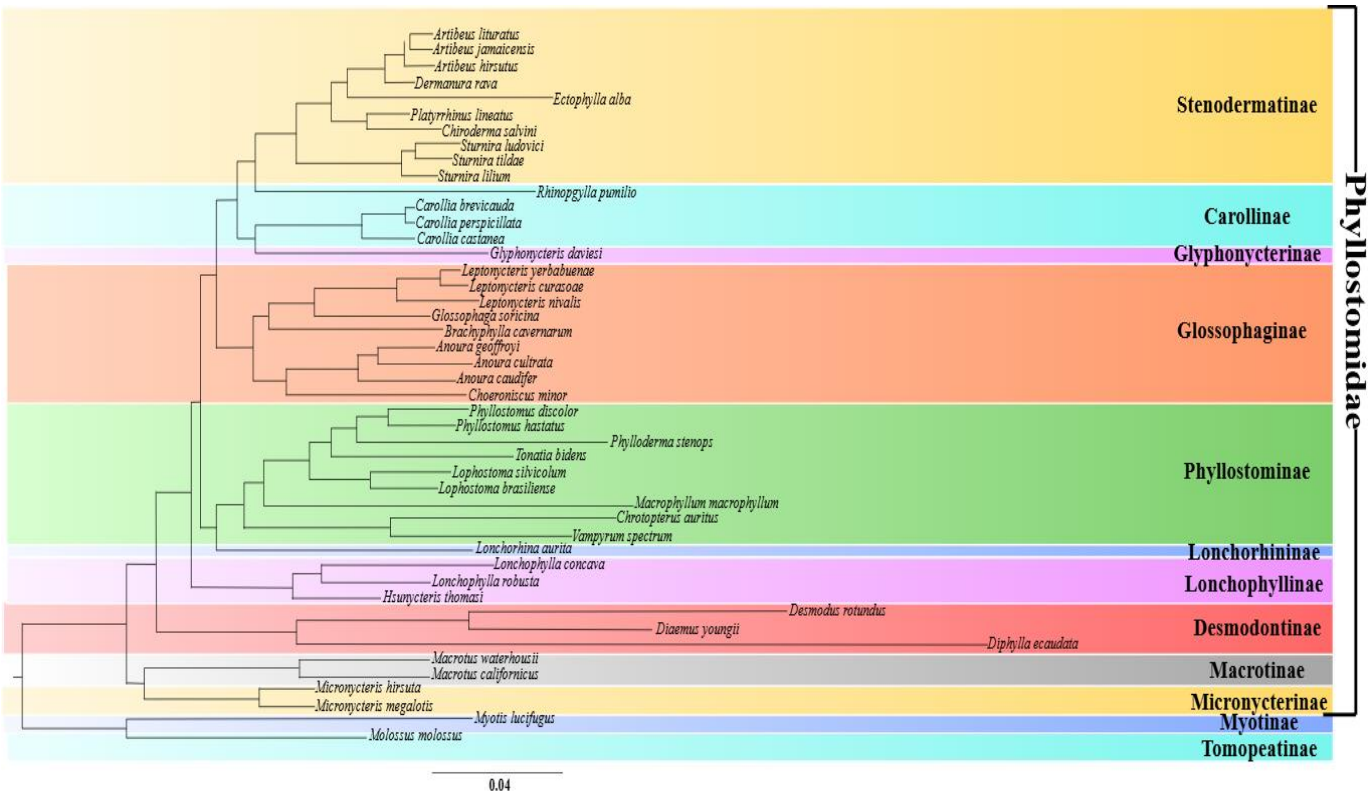


Fig. 5 Phylogenetic analysis showing the position of *Artibeus hirsutus* in relation to other taxa in the family Phyllostomidae with available mitochondrial genomes. Phylogenetic tree generated using maximum-likelihood analysis based on the 13 mitochondrial protein-coding genes.